



*Dedicated to Professor Zeno Simon  
on the occasion of his 80<sup>th</sup> anniversary*

## THE EFFECT OF PROCAINE ON LIPID DOMAINS INVESTIGATED BY CONTACT MODE ATOMIC FORCE MICROSCOPY

Petre T. FRANGOPOL,<sup>a,b</sup> David Allan CADENHEAD,<sup>c</sup> Gheorghe TOMOAI, <sup>d</sup>  
Aurora MOCANU<sup>a</sup> and Maria TOMOAI-COTISEL<sup>a,\*</sup>

<sup>a</sup>Babes-Bolyai University of Cluj-Napoca, Faculty of Chemistry and Chemical Engineering, Physical Chemistry Center,  
11 Arany J. Str., 400028 Cluj-Napoca, Roumania

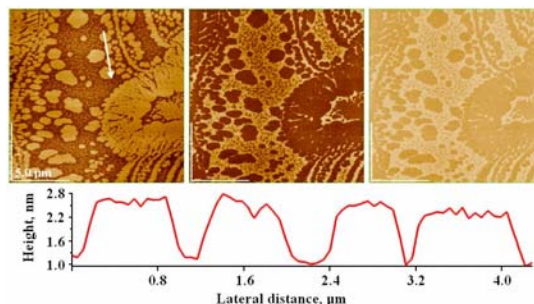
<sup>b</sup>Horia Hulubei National Institute of Research and Development for Nuclear Physics, 30 Reactorului Str., P.O. Box MG-6, 077125  
Măgurele-Ilfov, Roumania

<sup>c</sup>State University of New York at Buffalo, Department of Chemistry, 410 NSC, 14260-3000 Buffalo, NY, USA

<sup>d</sup>Iuliu Hatieganu University of Medicine and Pharmacy, Orthopaedics and Traumatology Department, 47 Traian Mosoiu Str.,  
400132 Cluj-Napoca, Roumania

*Received November 5, 2014*

Langmuir-Blodgett (LB) monolayers made of L- $\alpha$ -dipalmitoyl phosphatidylcholine (DPPC) without or in the presence of procaine were employed for mimicking cell membranes and were investigated by contact mode atomic force microscopy (cm-AFM). The structure and properties of different lipid phases induced by procaine were evidenced for the first time by using topography, friction force (FF) and force modulation (FM) images, simultaneously obtained with cm-AFM. In addition, both FF and FM images allow the edge-enhanced imaging of any lipid domain surface. The results indicate that procaine interacts with DPPC monolayers, stabilizes the lipid membrane interface and induces condensed lipid domain formation, modulating membrane functional properties. The procaine effect on lipid domains is also important for the emergence of lateral membrane heterogeneity and can intervene in the generation process of anesthesia. We further suggest that cm-AFM can be used for the scanning of LB monolayers to fully characterize the structure of self-assembled lipid domains and especially lipid domain boundaries within heterogeneous membranes.



### INTRODUCTION

It is recognized that the interaction of local anesthetics with membranes lead to changes in membrane lipid domains<sup>1-4</sup> disturbing the specific trans-membrane proteins of the ionic channels and

thus, blocking the nerve signal propagation.<sup>5,6</sup> It is documented that the anesthetic action on membranes<sup>7-12</sup> is primarily caused by the distribution of local anesthetics within lipid membranes.

Among local anesthetics, procaine hydrochloride, known also as novocaine, is frequently used.

\* Corresponding author: [mcotisel@chem.ubbcluj.ro](mailto:mcotisel@chem.ubbcluj.ro)

However, due to the complexity of biological membranes, procaine effects are not yet fully understood and thus, the influence on lipid membrane models is thus under current investigation.<sup>1-3, 9, 11, 12</sup>

Recently, the procaine binding to the membrane surface of human erythrocytes was evidenced by atomic force microscopy in tapping mode (tm-AFM),<sup>3</sup> due to the AFM high sensitivity to small height variations in the surface, at nanometer scale.<sup>13-20</sup> The alteration in the surface morphology of erythrocyte membrane has been associated with the lipid domain formation,<sup>3</sup> induced by procaine within the cell surface, and it is in substantial agreement with hypotonic hemolytic measurements coupled with electron micrographs.<sup>4</sup>

As a model for biological membranes, Langmuir lipid monolayers have been used, spread at the air/water interfaces as monomolecular insoluble films, or transferred from water on solid surface.<sup>1, 2, 13-16</sup> Early pioneering work has demonstrated that the anesthetics expand the lipid monolayers, at low and intermediate lateral surface pressures, depending on the experimental conditions, such as anesthetic concentration, surface properties of the chosen lipid and anesthetic compound, aqueous phase pH and ionic strengths.<sup>21-44</sup> The expanding effect can occur from various possible reasons, such as anesthetic adsorption on lipid monolayers, its binding and penetration into the lipid phase,<sup>30, 31, 34, 37-39</sup> modifying the structure of lipid domains.<sup>37-44</sup>

By using fluorescence microscopy,<sup>38</sup> we examined L- $\alpha$ -dipalmitoyl phosphatidylcholine (DPPC) and procaine monolayers, self-assembled directly on air/water interface, and we evidenced the effects of procaine on the lipid phase transition from the liquid expanded (LE) to liquid condensed (LC).<sup>30, 37-39</sup> The fluorescence images revealed a preferential location of adsorbed procaine molecules at the border between the LE and LC phases, reducing the line tension between the lipid phases.<sup>38</sup>

Additionally, the domain structure of lipid monolayers, at the phase transition in the absence and the presence of procaine, was recently investigated by tapping mode AFM, tm-AFM<sup>1,2</sup> on transferred lipid monolayers, from the air/water interface, on mica surface by Langmuir-Blodgett (LB) technique.<sup>1,2, 13-16</sup> Coexistence of liquid condensed (LC), called also tilted condensed<sup>45</sup>, and liquid expanded (LE) phases has been observed for the lipid monolayers.<sup>1,2, 38, 45</sup>

The goal of this work is to further examine the structure of DPPC monolayers at the phase

transition, from liquid expanded to liquid condensed, when procaine is incorporated at room temperature. Using for the first time contact mode AFM (cm-AFM), the topographical data were obtained simultaneously with friction force (FF) images and force modulation (FM) images for mixed DPPC and procaine monolayers. These cm-AFM images provide the direct evidence so far for the structure of the domain boundary between the LE and LC phases in the DPPC and procaine monolayers deposited on mica. These data can contribute to the understanding of the molecular mechanism of procaine action, particularly in interfacial phenomena that occur at the biological membrane level in anesthesia.

## RESULTS AND DISCUSSION

### DPPC monolayers and 2D topographies

DPPC monolayers without as well as in the presence of procaine were transferred at 8 mN/m from water to mica by Langmuir-Blodgett technique, as reported elsewhere.<sup>1, 2</sup> The 2D topographic images of pure DPPC monolayers as well as of mixed DPPC and procaine monolayers, obtained on 0.001 M procaine in aqueous solution, are shown in Figs. 1.1 and 1.3, respectively. Topography of each monolayer shows heterogeneous lipid domains with two distinct lipid (LC and LE) phases of rather smooth flat surface (see Table 1), as judged by the roughness, given as root mean square (RMS) values.<sup>3, 17, 18</sup> The RMS values are very low for these LB samples (Table 1), when calculated either on scanned areas or on cross section profiles. Similar results for lipid layers were also reported previously by using tm-AFM<sup>1,2</sup> and are in substantial agreement with reported data<sup>14</sup> under appropriate conditions. Therefore, it is demonstrated that the DPPC layers are stable and can be scanned with cm-AFM.

Although the height difference of lipid domains is quite small as shown in cross section profiles for these LB monolayers (Figs. 1.2 and 1.4), large LC domains and small size LC domains are observed (bright areas) in both topographies given in Figs. 1.1 and 1.3. Therefore, various lateral sizes of LC domains are identified from nano size to several  $\mu\text{m}$  for pure DPPC monolayers and reaching 15 or 20  $\mu\text{m}$  for mixed DPPC and procaine monolayers. These LC domains are surrounded by a lower LE matrix that contains numerous small condensed

domains with height of about  $2.2 \text{ nm} \pm 0.3 \text{ nm}$ , estimated for pure DPPC monolayers (Fig. 1.2), and about  $3.7 \text{ nm} \pm 0.4 \text{ nm}$ , obtained for mixed DPPC and procaine monolayers (Fig. 1.4). Thus, the addition of procaine resulted in its binding to DPPC molecules and an increase in the height of lipid domains is observed (Fig. 1.4).

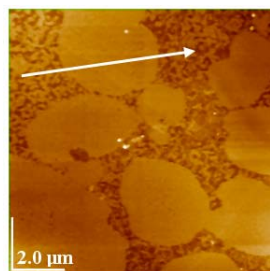
It is to be noted that the maximum height of  $4.1 \text{ nm} \pm 0.1 \text{ nm}$  (Fig. 1.4), also found for LC domains within mixed DPPC and procaine monolayers, coincides with the calculated height for DPPC molecules, well packed in a hexagonal DPPC lattice, which can be realized near the collapse of DPPC monolayers.<sup>50</sup> This fact proves that lipid LC domains are merged into larger condensed areas in the presence of procaine during the compression of the mixed DPPC and procaine monolayers to the collapse, where a highly packed lipid LC phase is realized.<sup>30,38</sup>

The LC phase is recognized to be formed by ordered DPPC molecules organized in tilted condensed liquid as identified by X-ray measurements.<sup>45</sup> At the lipid phase transition, these LC domains are surrounded by the lower domains of LE phase, where DPPC molecules are considered to form a liquid disordered phase,<sup>45</sup> or another more tilted phase as judged by AFM and force spectroscopy.<sup>14</sup> In consequence, at the phase transition from LE to LC, a mosaic of the two lipid (LC and LE) phases can coexist within pure DPPC monolayers. From thermodynamic point of view, the LE to LC phase transition is a first order transition and it is approximated on the compression isotherms of DPPC monolayers by a kink,<sup>30, 31, 45, 50</sup> at  $8 \text{ mN/m}$  for pure DPPC monolayers. Then, this is followed by an intermediary liquid<sup>45, 50</sup> which is formed by a mosaic of LE and LC lipid domains.<sup>1, 2, 30, 38</sup>

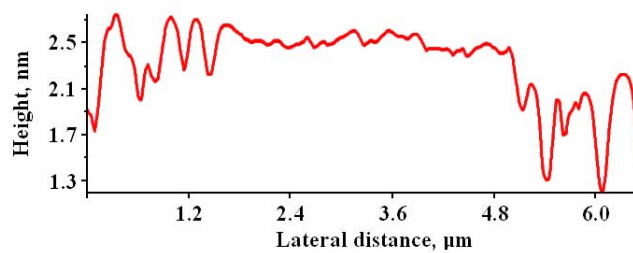
Table 1

Surface roughness, RMS values in nm, for pure DPPC monolayers and for mixed DPPC and procaine monolayers at specified scanned area of LB monolayers and on cross section profile, with corresponding figures

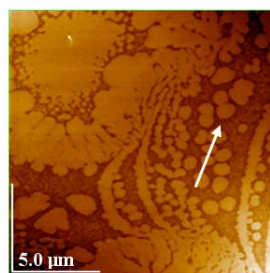
LB monolayer	Scanned area	RMS on area, nm	Figs.	RMS on cross profile, nm	Figs.
DPPC	$10 \mu\text{m} \times 10 \mu\text{m}$	$0.50 \pm 0.12$	1.1	$0.38 \pm 0.05$	1.2
	$2.6 \mu\text{m} \times 2.6 \mu\text{m}$	$0.43 \pm 0.10$	2.1	$0.43 \pm 0.10$	2.4
	$1.7 \mu\text{m} \times 1.7 \mu\text{m}$	$0.39 \pm 0.10$	2.5	$0.42 \pm 0.10$	2.8
DPPC and procaine	$15 \mu\text{m} \times 15 \mu\text{m}$	$0.86 \pm 0.21$	1.3	$0.52 \pm 0.10$	1.4
	$15 \mu\text{m} \times 15 \mu\text{m}$	$0.63 \pm 0.14$	3.1	$0.57 \pm 0.10$	3.4
	$10 \mu\text{m} \times 10 \mu\text{m}$	$0.55 \pm 0.15$	3.5	$0.42 \pm 0.10$	3.8
	$2 \mu\text{m} \times 2 \mu\text{m}$	$0.44 \pm 0.10$	3.9	$0.38 \pm 0.05$	3.12



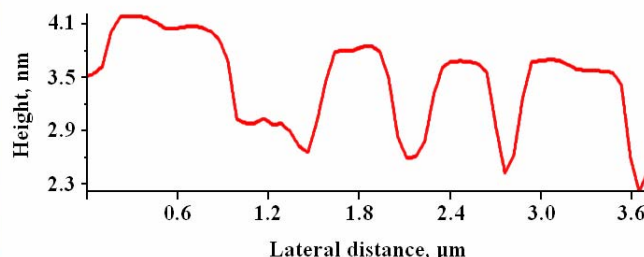
(1.1)



(1.2)



(1.3)



(1.4)

Fig. 1 – Contact mode AFM (cm-AFM) images. Pure DPPC monolayer transferred on mica surface: topography (1.1), scanned area  $10 \mu\text{m} \times 10 \mu\text{m}$ ; cross section profile (1.2), along the arrow given in Fig. 1.1; mixed DPPC and procaine monolayer on mica: topography (1.3), scanned area  $15 \mu\text{m} \times 15 \mu\text{m}$ ; cross section profile (1.4), along the arrow given in Fig. 1.3.

It is recognized that the investigation of the lipid domain formation in model membranes is important for a better understanding of membrane structural changes related to interfacial phenomena which occur during anesthesia. Therefore, additional examples are specifically shown for pure DPPC monolayers (Fig. 2) and for the mixed DPPC and procaine monolayers (Fig. 3), for different scanned areas. The cm-AFM images show contrast between lipid phases through the differences in height (2D-topographies), in friction force (*i.e.*, FF images) and in mechanical

properties (*i.e.*, using force modulation, FM images) of the co-existing phases as observed in Figs. 2 and 3.

### Height contrast between the DPPC phases

The phase separation is clearly observed in Figs. 1-3, due to the difference in height of the two (LC and LE) phases for pure DPPC monolayers and for the DPPC and procaine mixture.

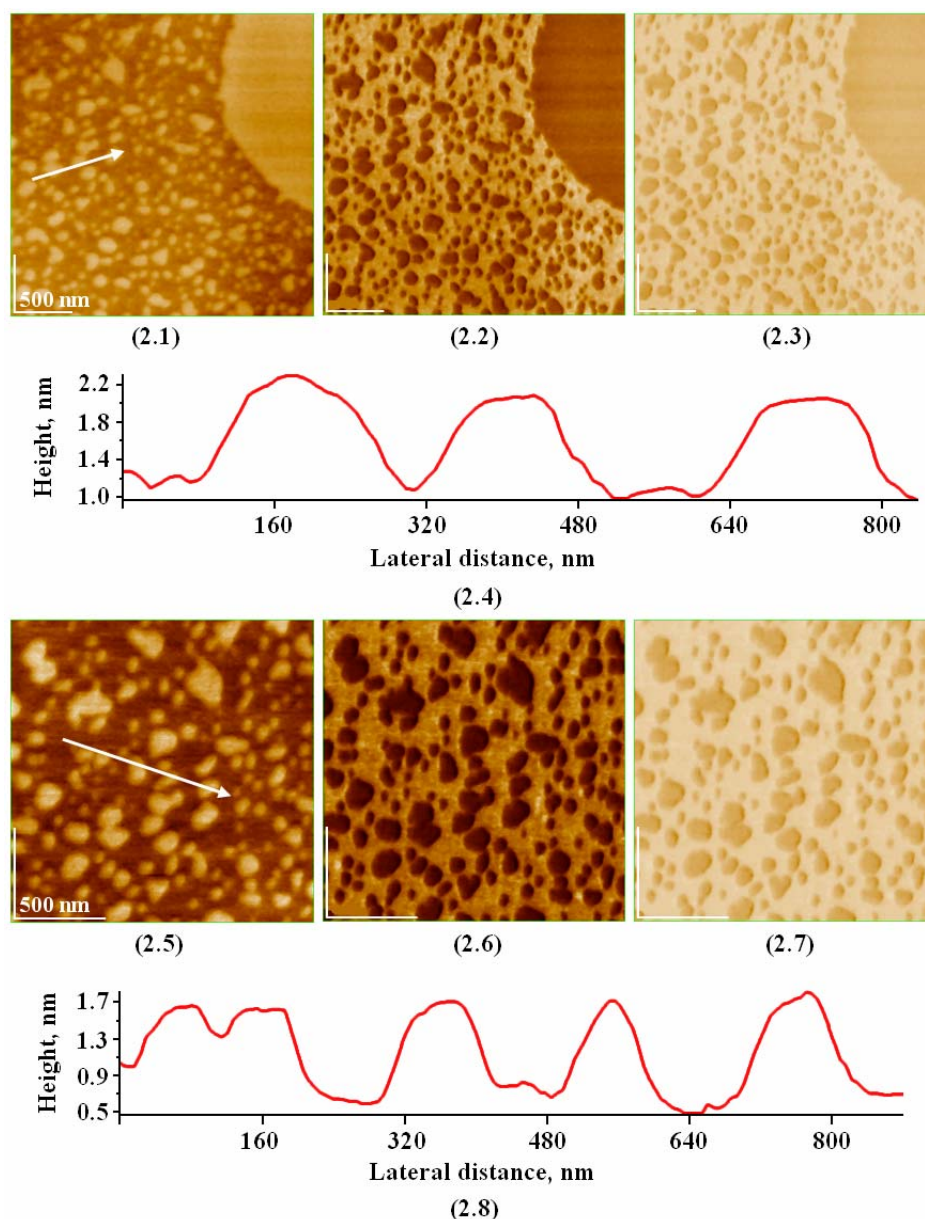


Fig. 2 – The cm-AFM images for pure DPPC monolayer: topographic (height) image (2.1), scanned area  $2.6 \mu\text{m} \times 2.6 \mu\text{m}$ ; friction force (FF) image (2.2); force modulation (FM) image (2.3); cross section profile (2.4), along the arrow given in Fig. 2.1; topographic image (2.5), scanned area  $1.7 \mu\text{m} \times 1.7 \mu\text{m}$ ; FF image (2.6); FM image (2.7); cross section profile (2.8), along the arrow given in Fig. 2.5.

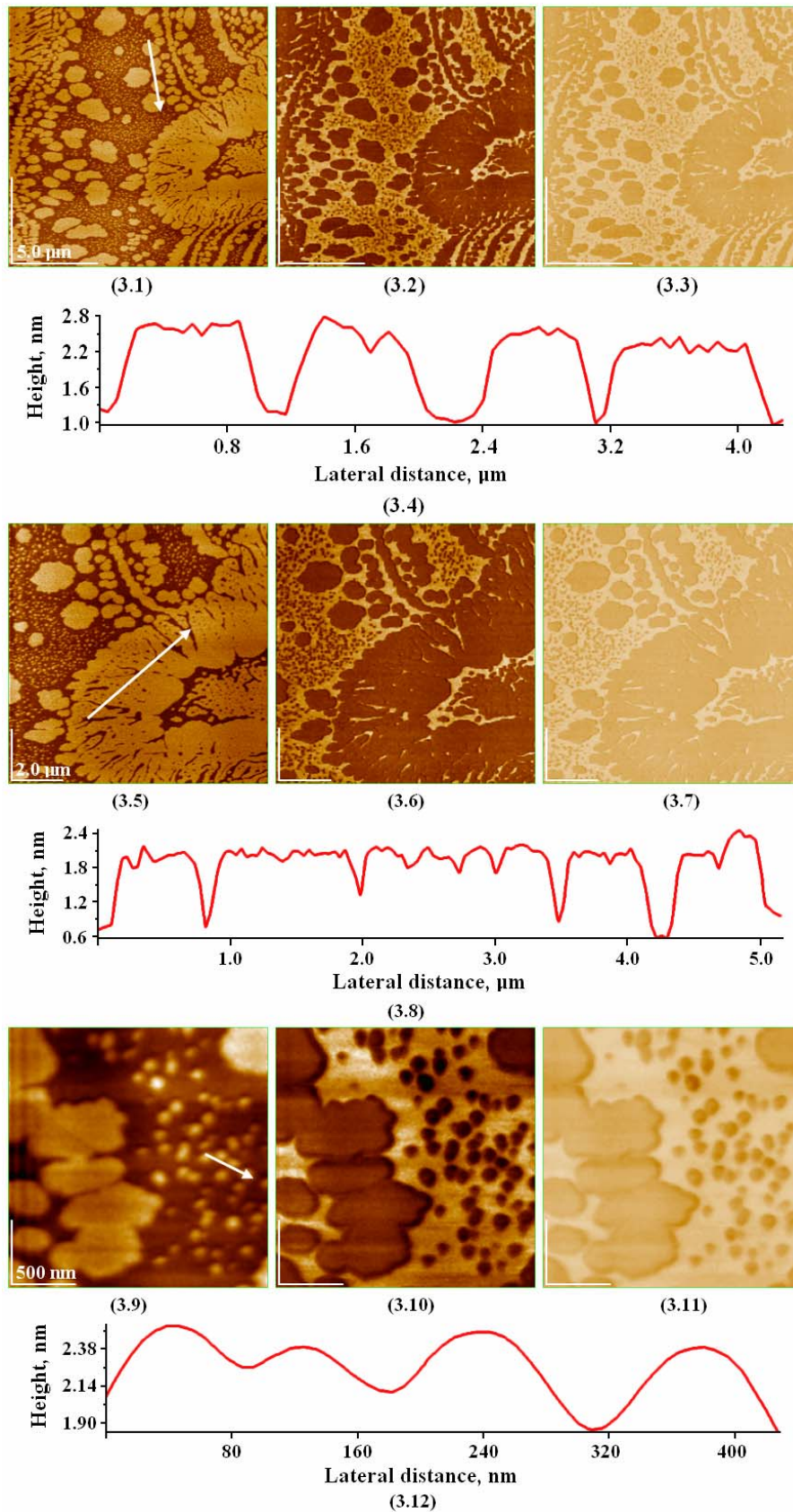


Fig. 3 – The cm-AFM images for mixed DPPC and procaine monolayer: topographic image (3.1), scanned area  $15\ \mu\text{m} \times 15\ \mu\text{m}$ ; FF image (3.2); FM image (3.3); cross section profile (3.4), along the arrow given in Fig. 3.1; topographic image (3.5), scanned area  $10\ \mu\text{m} \times 10\ \mu\text{m}$ ; FF image (3.6); FM image (3.7); cross section profile (3.8), along the arrow given in Fig. 3.5; topographic image (3.9), scanned area  $2\ \mu\text{m} \times 2\ \mu\text{m}$ ; FF image (3.10); FM image (3.11); cross section profile (3.12), along the arrow given in Fig. 3.9.

In the case of DPPC pure monolayers, LC areas (Figs. 1.1, 2.1 and 2.5) are discrete, round or oval domains (Fig. 1.1), almost uniform in height ( $2.2 \pm 0.3$  nm, shown in Fig. 1.2), with height of  $2.1 \pm 0.2$  nm (Fig. 2.4) and with height of  $1.8 \pm 0.2$  nm (Fig. 2.8). Interestingly, the difference in height of LC and LE domains is almost constant of about  $1.1 \pm 0.2$  nm, which is practically independent of the size of scanned areas for DPPC pure monolayers. These results are in substantial agreement with the known remarks that lipids form a continuous layer and the height differences generally observed are of about 1 nm height steps between ordered and disordered phases.<sup>16</sup>

For the mixed DPPC and procaine monolayers, a mosaic of various LC and LE domains is identified in Figs. 1.3, 3.1, 3.5 and 3.9, for different sample scanned areas. The LC domains are distinct of various lateral sizes and different shapes (Figs. 1.3, 3.1, 3.5 and 3.9). The DPPC and procaine interactions are primarily important for the emergence of lateral membrane heterogeneity to large LC areas up to 15 or even 20  $\mu\text{m}$  (Figs. 1.3 and 3.1) at the surface pressure of 8 mN/m. This effect of procaine can be rationally interpreted by procaine's ability to induce firstly the self assembling of DPPC molecules in rather small LC domains (as observed directly on water with fluorescence microscopy<sup>38</sup>). After that, procaine generates further assembling into larger ordered LC domains. Evidently, the LC domains have a particular wrinkled nanostructure (*e.g.*, Figs. 3.5 and 3.8), due to an incomplete two-dimensional packing<sup>51</sup> within the boundaries of lipid domains. Consequently, it is possible to affirm that the nanostructured lipid condensed domains found in mixed DPPC and procaine monolayers are larger than those identified in pure DPPC monolayers for the same scanned sample areas.

The height difference is almost constant  $1.6 \pm 0.3$  nm, as given in Figs. 1.4, 3.4 and 3.8, between highly ordered and disordered phases in mixed DPPC and procaine monolayers. Occasionally, a height step of about  $1.2 \pm 0.2$  nm can also be observed as it is the case given in Fig. 3.12, probably due to the tip-convolution effects for the smallest lipid domains. However, it is reasonable to generally say that the height step in mixed monolayers is higher than those found in the pure DPPC monolayers, due to the specific interactions between lipid and procaine also reported earlier.<sup>1, 2, 30, 34, 38</sup>

It is not surprising that the step, found in the height difference between LC domains and LE

domains, is the same and independent of the size of scanned sample area. This demonstrates a lack of adhesion between the cm-AFM tip and LC domains or LE domains at scanning the lipid domain boundaries, also indicating the capability of cm-AFM in imaging the lipid domains of significant heterogeneity, with high resolution.

### Friction and force modulation contrast between DPPC phases

In cm-AFM, the vertical deflection of the cantilever is used for topographic images to control the height of the monolayer. Topographic data are collected independently from local variations in elastic properties or in friction characteristics of different lipid domains. Simultaneously, the lateral deflection of the cantilever can be measured, due to the friction force between the cantilever tip and the surface of the LB-monolayer. Certainly, the friction contrast in friction force (FF) image can indicate the differences in chemical properties and in the structure of the monolayer phases. At the same time, force modulation (FM) images are also obtained and are related generally to the elastic properties and relative stiffness of the surface of lipid domains. The variation in the amplitude of cantilever deflection at the frequency of force modulation might be considered as a measure of the relative stiffness of the surface. Accordingly, all three types of images were collected simultaneously having a direct correlation between topographic structure, elastic and friction properties of lipid phases.

For example, Figs. 2.1, 2.2 and 2.3 were obtained simultaneously. The topography (Fig. 2.1), the FF image (Fig. 2.2) and FM image (Fig. 2.3) for pure DPPC monolayers are given at a scanned area of  $2.6 \mu\text{m} \times 2.6 \mu\text{m}$ . These images are also given for a scan area of  $1.7 \mu\text{m} \times 1.7 \mu\text{m}$  (Figs. 2.5-2.7). Further, it is to be mentioned that the FF images and the FM images present a high contrast (independent of scanned areas) describing in details the structure of LC and LE domains and the domain boundaries, where the height sharply changes.

Further, several examples are shown for the mixed DPPC and procaine monolayers (Fig. 3), for different scanned areas. The FF images (Figs. 3.2, 3.6 and 3.10) prove that the procaine addition leads to complex heterogeneous surface of mixed DPPC and procaine monolayers, showing also in detail the structure of both LC and LE phases. In addition, the boundary structure of lipid domains is clearly observed.

Furthermore, the FM images (Figs. 3.3, 3.7 and 3.11) present a clear difference between the morphology of lipid phases and primarily show the lipid boundary structure, similarly with FF images. However, the interpretation of mechanical properties of lipid domains is a complex subject that we will attempt to develop in the future by measuring the force curves in cm-AFM.

The obtained results with cm-AFM are in substantial agreement with previously published data using tm-AFM for the characterization of DPPC phase behavior.<sup>1,2</sup> In addition, the FF and FM images also disclose the fine structure of edged boundaries of lipid domains, evidencing various actions of procaine on lipid domains. Consequently, both FF images and FM images are essential adding valuable structural and morphological data to the description of lipid domains in monolayers, used as an important model for mimicking the biological membranes.

## EXPERIMENTAL

### Materials

L- $\alpha$ -Dipalmitoyl phosphatidylcholine (DPPC) was purchased from Avanti Polar Lipids (Alabaster, AL). Procaine hydrochloride was obtained from Merck (Darmstadt, Germany). All chemicals were of analytical grade and were used without further purification. Procaine was dissolved in twice-distilled water for the concentration of 0.001 M, at pH 5.6. This concentration of procaine was used since it was earlier demonstrated to produce a substantial effect on lipid domains<sup>1, 2, 38</sup>. All glassware was cleaned with a fresh solution of HNO<sub>3</sub>/HCl (3:1, v/v) or with sulfochromic solution, rinsed thoroughly with pure water, and dried before use.

### Langmuir and Langmuir-Blodgett monolayers

The preparation of Langmuir and Langmuir-Blodgett (LB) monolayers was presented elsewhere.<sup>1,2</sup> Briefly, DPPC was dissolved in a mixture of chloroform and ethanol (9:1, v/v), obtaining a 1 mM lipid in organic solution. By spreading the DPPC organic solution on water, Langmuir films were prepared in the Langmuir-Blodgett equipment (KSV 5000, Finland), in the absence and in the presence of procaine in aqueous solution. After the spreading of Langmuir DPPC monolayer, the compression isotherm, in terms of surface pressure versus mean area of DPPC molecule, was recorded with a constant compression speed of 10 mm/min, as earlier reported.<sup>1,2</sup> For cm-AFM observations, a single layer of pure DPPC or of a DPPC and procaine mixture was transferred from water to freshly cleaved mica surface using a vertical dipping method at a constant surface pressure of 8 mN/m, which is characteristic for DPPC phase transition at room temperature. The transferred layers on mica are named LB monolayers. The transfer for LB monolayers took place at a rate of about 5 mm/min.

### AFM observations

AFM is a surface imaging technique with a nanometer scale, high resolution<sup>46-49</sup>. AFM investigation on LB monolayers of pure DPPC as well as on DPPC and procaine mixture was performed in contact (repulsive) mode (cm-AFM) in air using the AFM 4210 JEOL, Japan. The cm-AFM images were analyzed by using AFM JEOL software. A scanner with maximum scan areas of 30  $\mu\text{m}$  x 30  $\mu\text{m}$  was used. The cantilevers were fabricated by Budget Sensors, Sofia, Bulgaria, with silicon nitride tips, of typical curvature radius smaller than 10 nm, and with a spring constant of either 60 mN/m or of 200 mN/m. They were vibrated at their resonant frequency of about 13 kHz. Ten LB samples were independently prepared for each monolayer and at least five separate areas were imaged for each sample. The imaging force was between 0.5 and 1 nN, and the scan rate was typically of 1 Hz. No attempt was made to account for tip-convolution effects for the smaller domains. For each LB sample, several areas were scanned from 20  $\mu\text{m}$  x 20  $\mu\text{m}$  to 1  $\mu\text{m}$  x 1  $\mu\text{m}$ .

### Surface roughness

In order to analyze the monolayer surface, the roughness of the LB monolayers was determined as the root mean square (RMS) value of the height distribution:

$$\text{RMS} = \sqrt{\frac{\sum_{i=1}^N (z_i - z_m)^2}{(N-1)}}$$

where  $z_i$  is the height of  $i^{\text{th}}$  point,  $z_m$  represents the mean height and  $N$  is the total number of data points in the scanned area.<sup>3, 17, 18</sup> By definition, the surface roughness is a morphology related parameter.

## CONCLUSIONS

The data reported here illustrate the importance of cm-AFM imaging to characterize the phase behavior of pure lipid monolayers and mixed monolayers of lipid with different biocompounds, such as the local anesthetic procaine. The mixed monolayers of DPPC and procaine can serve as a useful membrane model for the investigation of interfacial phenomena involved in molecular mechanism of anesthesia.

The cm-AFM offers three different ways of observing contrast between lipid phases from differences in height, friction and mechanical properties. Thus, topography, friction force and force modulation images, obtained with cm-AFM, revealed the densely packed (LC) domains in coexistence with expanded (LE) domains at the lipid phase transition, which was found at 8 mN/m.<sup>1, 2, 30, 38, 50</sup> Also, the effect of procaine on the lipid domains emerging the LC domains into larger nanostructured areas is determined in relationship with procaine adsorption and its binding and penetration into these lipid self assemblies.

In addition, cm-AFM demonstrates to have the ability to reveal the domain boundaries of different lipid patches, within their self-organization. These data support the structure of lipid domains, which might be critical in different cell processes, such as anesthesia, molecular recognition, signaling, endocytosis or exocytosis.

Certainly, cm-AFM can be also combined with tm-AFM, namely with topography, phase and amplitude images,<sup>1,2</sup> to jointly reveal the phase transition of lipid monolayers without or in the presence of drugs to better understand the structure and the properties of natural membranes. AFM force spectroscopy is under current examination in our laboratory to directly measure the mechanical properties, e.g., Young's modulus, of lipid domains in the presence of various drugs.

*Acknowledgments:* The support of UEFISCDI, through grant No. 257, is gratefully acknowledged.

## REFERENCES

- P. T. Frangopol, D. A. Cadenhead, M. Tomoaia-Cotisel and A. Mocanu, *Studia, Univ. Babeş-Bolyai, Chem.*, **2009**, *54*, 23.
- M. Tomoaia-Cotisel and A. Mocanu, *Rev. Chim. (Bucharest)*, **2008**, *59*, 1230.
- U. V. Zdrengea, Gh. Tomoaia, D. V. Pop-Toader, A. Mocanu, O. Horovitz and M. Tomoaia-Cotisel, *Combinatorial Chemistry & High Throughput Screening*, **2011**, *14*, 237.
- P. Seeman, *Biochem. Pharmacol.*, **1966**, *15*, 1753.
- Z. V. Leonenko and D. T. Cramb, *Can. J. Chem.*, **2004**, *82*, 1128.
- A. N. Bondar, S. Suhai, J. C. Smith and P. T. Frangopol, *Romanian Reports in Physics*, **2007**, *59*, 289.
- H. Tsuchiya, M. Mizogami, T. Ueno and K. Takakura, *Inflammopharmacol.*, **2007**, *15*, 164.
- Z. Leonenko, E. Finot and D. Cramb, *Biochim. Biophys. Acta*, **2006**, *1758*, 487.
- T. Hata, H. Matsuki and S. Kaneshina, *Colloids Surf. B.*, **2000**, *18*, 41.
- H. Matsuki, S. Kaneshina, H. Kamaya and I. Ueda, *J. Phys. Chem. B*, **1998**, *102*, 3295.
- H. Matsuki, M. Yamanaka, H. Kamaya, S. Kaneshina and I. Ueda, *Colloids Surf. B.*, **2004**, *38*, 91.
- M. E. Barbinta-Patrascu, L. Tugulea and A. Meghea, *Rev. Chim. (Bucharest)*, **2009**, *60*, 337.
- Z. V. Leonenko, E. Finot, H. Ma, T. E. S. Dahms and D. T. Cramb, *Biophys. J.*, **2004**, *86*, 3783.
- G. Oncins, L. Picas, J. Hernandez-Borrell, S. Garcia-Manyes and F. Sanz, *Biophys. J.*, **2007**, *93*, 2713.
- C. Yuan and L. J. Johnston, *Biophys. J.*, **2001**, *81*, 1059.
- M. Deleu, K. Nott, R. Brasseur, P. Jacques, P. Thonart and Y.F. Dufrene, *Biochim. Biophys. Acta*, **2001**, *1513*, 55.
- Y. Wu, Y. Hu, J. Cai, S. Ma, X. Wang and Y. Chen, *Scanning*, **2008**, *30*, 426.
- M. Girasole, G. Pompeo, A. Cricenti, A. Congiu-Castellano, F. Andreola, A. Serafino, B. H. Frazer, G. Boumis and G. Amiconi, *Biochim. Biophys. Acta*, **2007**, *1768*, 1268.
- Y. Chunbo, D. Desheng, L. Zuhong and L. Juzheng, *Colloids Surf. A.*, **1999**, *150*, 1.
- M. H. Greenhall, P. J. Lukes, M. C. Petty, J. Yarwood and Y. Lvov, *Thin Solid Films*, **1994**, *243*, 596.
- M. Tomoaia-Cotisel, E. Chifu, A. Mocanu, J. Zsakó, M. Salajan and P. T. Frangopol, *Rev. Roum. Biochim.*, **1988**, *25*, 227.
- M. Tomoaia-Cotisel, J. Zsakó, E. Chifu, P.T. Frangopol, W.A.P. Luck and E. Osawa, *Rev. Roum. Biochim.*, **1989**, *26*, 305.
- J. Zsakó, M. Tomoaia-Cotisel, E. Chifu, A. Mocanu and P. T. Frangopol, *Biochim. Biophys. Acta*, **1990**, *1024*, 227.
- J. Zsakó, M. Tomoaia-Cotisel, E. Chifu, I. Albu, A. Mocanu and P. T. Frangopol, *Rev. Roum. Chim.*, **1990**, *35*, 867.
- E. Chifu, M. Tomoaia-Cotisel, J. Zsakó, I. Albu, A. Mocanu and P. T. Frangopol, *Rev. Roum. Chim.*, **1990**, *35*, 879.
- M. Tomoaia-Cotisel, E. Chifu, S. Jitian, I. Bratu, S. Bran, P. T. Frangopol and A. Mocanu, *Stud. Univ. Babeş-Bolyai, Chem.*, **1990**, *35*, 17.
- E. Chifu, M. Tomoaia-Cotisel, J. Zsakó, A. Mocanu, M. Salajan, M. Neag and P. T. Frangopol, "Seminars in Biophysics", Vol. 6, Editors: P. T. Frangopol and V. V. Morariu, IAP Press, Bucharest, 1990, p. 117.
- J. Zsakó, M. Tomoaia-Cotisel, I. Albu, A. Mocanu, E. Chifu and P.T. Frangopol, *Rev. Roum. Biochim.*, **1991**, *28*, 33.
- M. Tomoaia-Cotisel, E. Chifu, J. Zsakó, P. T. Frangopol, P. J. Quinn and A. Mocanu, *Stud. Univ. Babeş-Bolyai, Chem.*, **1993**, *38*, 81.
- J. Zsakó, M. Tomoaia-Cotisel, E. Chifu, A. Mocanu and P. T. Frangopol, *Gazz. Chim. Ital.*, **1994**, *124*, 5.
- J. Zsakó, E. Chifu, M. Tomoaia-Cotisel, A. Mocanu and P. T. Frangopol, *Rev. Roum. Chim.*, **1994**, *39*, 777.
- M. Tomoaia-Cotisel, J. Zsakó, E. Chifu, A. Mocanu, P. T. Frangopol and P. J. Quinn, *J. Romanian Colloid and Surface Chem. Assoc.*, **1997**, *2*, 30.
- M. Tomoaia-Cotisel, T. Oproiu, J. Zsakó, A. Mocanu, P. T. Frangopol and P. J. Quinn, *Rev. Roum. Chim.*, **2000**, *45*, 851.
- H. G. Coster, V. J. James, C. Berthet and A. Miller, *Biochim. Biophys. Acta*, **1981**, *641*, 281.
- P. T. Frangopol and D. Mihailescu, *Colloids Surf. B.*, **2001**, *22*, 3.
- T. Hianik, M. Fajkus, B. Tarus, P. T. Frangopol, V. S. Markin and D. F. Landers, *Bioelectrochem. Bioenergetics*, **1998**, *46*, 1.
- M. Tomoaia-Cotisel and D. A. Cadenhead, *Langmuir*, **1991**, *7*, 964.
- B. Asgharian, D. A. Cadenhead and M. Tomoaia-Cotisel, *Langmuir*, **1993**, *9*, 228.
- M. Tomoaia-Cotisel, *Progr. Colloid Polym. Sci.*, **1990**, *83*, 155.
- H. Matsuki, K. Shimada, S. Kaneshina, M. Yamanaka, H. Kamaya and I. Ueda, *Langmuir*, **1997**, *13*, 6115.
- S. Y. Choi, S. G. Oh and J. S. Lee, *Colloids Surf. B.*, **2001**, *20*, 239.
- A. Cavalli, G. Borissevitch, M. Tabak and O. N. Oliveira Jr., *Thin Solid Films*, **1996**, *284-285*, 731.
- D. M. Goodman, E. M. Nemoto, R. W. Evans and P. M. Winter, *Chem. Phys. Lipids*, **1996**, *84*, 57.

44. S. Y. Choi, S. G. Oh and J. S. Lee, *Colloids Surf. B.*, **2000**, *17*, 255.
45. V. M. Kaganer, H. Mohwald and P. Dutta, *Rev. Modern Phys.*, **1999**, *71*, 779.
46. Gh. Tomoaia, P. T. Frangopol, O. Horovitz, L. D. Bobos, A. Mocanu and M. Tomoaia-Cotisel, *J. Nanosci. Nanotechnol.*, **2011**, *11*, 7762.
47. K. Hoda, Y. Ikeda, H. Kawasaki, K. Yamada, R. Higuchi and O. Shibata, *Colloids Surf. B.*, **2006**, *52*, 57.
48. Gh. Tomoaia, L. B. Pop, I. Petean and M. Tomoaia-Cotisel, *Materiale Plastice*, **2012**, *49*, 48.
49. A. Mocanu, R. D. Pasca, Gh. Tomoaia, A. Avranas, O. Horovitz and M. Tomoaia-Cotisel, *J. Nanosci. Nanotechnol.*, **2012**, *12*, 8935.
50. M. Tomoaia-Cotisel, J. Zsako and E. Chifu, *Ann. Chim. (Rome)*, **1981**, *71*, 189.
51. H. An, M. R. Nussio, M. G. Huson, N. H. Voelcker and J. G. Shapter, *Biophys. J.*, **2010**, *99*, 834.

